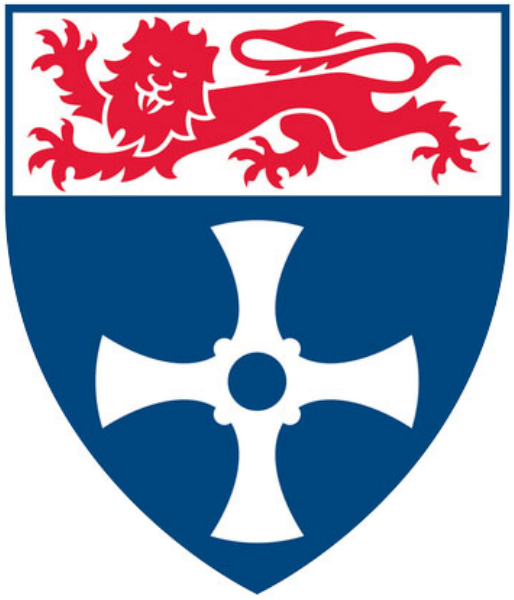

Newcastle University

Masters Project

Black Holes and Particle Orbits

Author:
Richard A.N. Smith

Supervisor:
Dr. David Toms

May 1, 2014

Abstract

Black holes are an important area of study because as our understanding of what they are and how they effect the matter around them increases, we can further our understanding of the universe and how it is shaped. They also provide a valuable test of Einstein's general relativity, and can produce a phenomenom known as gravitational lensing, which can help us view distant galaxies. In this paper we will introduce the Schwarzschild solution in general relativity and solve it exactly using Jacobi elliptic functions. We will solve the Schwarzschild metric using an approximate method, and use this to estimate perihelion precession. We will use approximate methods to solve the de Sitter-Schwarzschild metric and compare it to the Schwarzschild solution. We will introduce the Reissner-Nordström metric for charged black holes and use exact methods to solve it with Jacobi elliptic functions.

Contents

Chapter 1

Introduction

Research into Black Holes has become a huge part of modern physics and astronomy, but the ideas behind them have been around for centuries. The first idea that there could exist a body so massive that light could not escape was put forward by a geologist named Michell in 1783, cotained in a letter to the royal society. Independently, the famous French mathematician Laplace included the idea in a book which he published, in 1796. Although these ideas were proposed, they were generally ignored due to lack of understanding how light could be affected by gravity. This all changed in 1915 when Einstein released his theory of general relativity, which shows how gravity does influence the motion of light. Only a few months later Karl Schwarzschild found a solution for the gravitational field outside of a spherical mass, which is important for the idea of a black hole. It was not until 1967 that the term black hole was coined by physicist John Wheeler.

Black holes are created when a star runs out of fuel. At this point it will collapse upon itself into a small dense core, and if this core has a mass greater than approximately three times the mass of our Sun the force of gravity overwhelms all other forces and produces a black hole, as described in [2]. This extreme amount of matter packed into a very small area causes an unescapable gravitational field and the distance from which nothing may escape is known as the event horizon. At the centre of a black hole there lies a gravitational singularity. This is a region where the space-time curvature becomes infinite. This singular point has zero volume, but infinite density.

In general relativity we define particles travelling slower than the speed of light and particles travelling equal to the speed of light to be known repectively as time-like and null. There also exists particles which travel faster than the speed of light, known as space-like, but we shall not be considering them in this report. The main metrics for describing black holes are Schwarzschild, Reissner-Nordström and Kerr, with other variations on these available. In this report we will only be considering exact solutions for the Schwarzschild and Reissner-Nordström metrics due to time restraints. If an unfortunate observer crossed the event horizon of a Schwarzschild black hole there is nothing they could possibly do to escape, however we shall see that the Reissner-Nordström metric theoretically allows for inter-universal travel through black holes.

In this project we will be using Einstein's general theory of relativity to describe the behaviour of a particle outside a black hole. General relativity states that space and time are not seperate, and can be used together to create space-time. This space-time consists

of three physical dimensions and a fourth time dimension, and allows for curved space, as shown in figure 1.1. Black holes and the bending of light are often used as tests to prove general relativity in the science community. However due to their nature, black holes are extremely difficult to observe as they do not omit light, x-rays or other electromagnetic radiation. This means that conventional telescopes and detectors cannot directly find them. Instead, scientists look for matter behaving as we would expect it to around a black hole. If a cloud of matter or a star, passes near enough to a black hole, it will draw the matter inward in a process known as accretion.

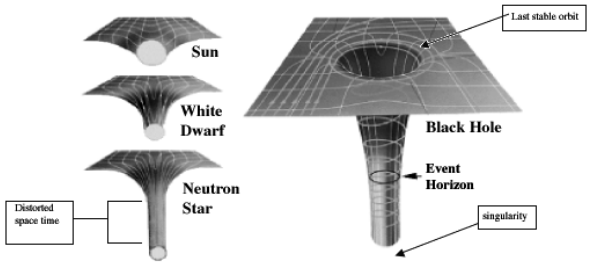

Figure 1.1: A diagram indicating how space-time bends with respect to different celestial bodies.
Image credit: Adam Apollo, http://scienceblogs.com/startswithabang/2012/05/10/why-youll-never-escape-from-a/

Knowing how objects orbit and behave around black holes is an important part of identifying and understanding them. Contrary to popular belief, black holes do not suck in all matter around them, they are celestial masses similar to a star which are capable of having orbiting bodies which may never pass the event horizon. There are two types of orbit a particle can have, known as bound or unbound respectively. Bound orbits remain in a fixed orbit similar to how planets in our solar system orbit the sun. Unbound orbits come from infinity but never achieve a stable orbit; they either proceed back to infinity or crash into the singularity. For both bound and unbound orbits we now define two seperate cases in the regions outside the event horizon and inside the event horizon, known as orbits of the first and second kind respectively.

Firstly we will then consider the exact solutions to Schwarzschild metric for all different orbits defined above. We shall also consider two special cases for the bound time-like geodesics. We will then consider the approximate solutions to the Schwarzschild and de Sitter-Schwarzschild metrics, and compare these to the post Newtonian approximation which we can define from our exact solution. Finally we will look at the Reissner-Nordström metric, which is similar to the Schwarzschild metric however it allows for the black hole to have a charge. We will talk about the interesting effects this metric allows, including two event horizons and travelling between universes through worm holes.

Throughout this report there will be visual representations of the orbits which we find which have been plotted in Maple.

Chapter 2

Schwarzschild Solution

2.1 The Schwarzschild Metric

In Einstein's theory of general relativity, the Schwarzschild solution describes the gravitational field around a spherical mass in a vacuum, with zero angular momentum, no electric charge and without a cosmological constant. The Schwarzschild solution is useful for mathematically predicting how objects behave outside of a black hole. These are known as 'Schwarzschild black holes', and are indestinguishable from each other except than by their respective mass. Firstly we must define the Schwarzschild metric in spherical polar coordinates, as seen in [1], which follows as

$$ds^2 = -d\tau^2 = -A(r)dt^2 + B(r)dr^2 - r^2\left(d\theta^2 + \sin^2\theta d\phi^2\right), \tag{2.1}$$

where $A(r) = F(r)$ and $B(r) = 1/F(r)$, and

$$F(r) = 1 - \frac{2M}{r}. \tag{2.2}$$

In this case we have used scaling to set both the gravitational constant and the speed of light to be equal to one. Using this value for $F(r)$ turns our line element into

$$d\tau^2 = \left(1 - \frac{2M}{r}\right)dt^2 - \left(1 - \frac{2M}{r}\right)^{-1}dr^2 - r^2\left(d\theta^2 + \sin^2\theta d\phi^2\right), \tag{2.3}$$

where;

- τ is the proper time,
- t is normal time,
- r is the radial coordiante,
- θ is the colatitudal angle,
- ϕ is the latitudal angle,
- M is the mass of the central object.

We can see that 2.3 breaks down when

$$F(r) = 0 \quad \text{i.e. when} \quad r = 2M. \tag{2.4}$$

We call this value of r the Schwarzschild radius, also known as the event horizon, r_s. This is the point where, once passed we can not return.

Using 2.3, and setting $\theta = \pi/2$ to define motion in a flat plane, which we can do as the solution is spherically symmetric, we can now aim to find a Lagrangian. Firstly we must define the two nescessary equations of motion to be

$$A(r)\dot{t} = E \tag{2.5}$$
$$r^2 \sin^2\theta\dot{\phi} = \ell, \tag{2.6}$$

where E is equivalent to energy and ℓ is angular momentum. Thus we can write the Lagrangian as

$$\begin{aligned} L &= -\frac{1}{2}F(r)\dot{t}^2 + \frac{1}{2F(r)}\dot{r}^2 + \frac{1}{2}r^2(\dot{\theta}^2 + \sin^2\theta\dot{\phi}^2) \\ &= -\frac{E^2}{2F(r)} + \frac{\dot{r}^2}{2F(r)} + \frac{\ell^2}{2r^2}. \end{aligned} \tag{2.7}$$

If a particle has non-zero mass at rest, its motion follows a time-like geodesic. If we choose the derivatives in 2.7 to be with respect to proper time, we can see that $L = -1/2$. For a particle with zero rest mass, for instance light particles, the motion follows a null geodesic relating to $d\tau^2 = 0$, giving $L = 0$. Thus we can now rearrange 2.7 to be

$$\dot{r}^2 = E^2 - \frac{\ell^2 F(r)}{r^2} + 2LF(r). \tag{2.8}$$

where

$$L = \begin{cases} -\frac{1}{2} \text{ if particle has non-zero rest mass} \\ 0 \text{ if particle has zero rest mass} \end{cases} \tag{2.9}$$

To help solve these equations we now introduce a new variable

$$u = \frac{1}{r} \tag{2.10}$$

Upon differentiation we find

$$\dot{r} = -\frac{\dot{u}}{u^2}, \tag{2.11}$$

and, using the chain rule, we can see

$$\dot{u} = \frac{\mathrm{d}u}{\mathrm{d}\phi}\frac{\mathrm{d}\phi}{\mathrm{d}\tau}. \tag{2.12}$$

$$\tag{2.13}$$

We have already seen from 2.6 with $\theta = \pi/2$ that $\dot{\theta} = \ell u^2$. Therefore we get,

$$\dot{u} = \ell u^2 \frac{\mathrm{d}u}{\mathrm{d}\phi} \tag{2.14}$$

and

$$\dot{r} = -\ell \frac{\mathrm{d}u}{\mathrm{d}\phi}. \tag{2.15}$$

Substituting these results into 2.7 and rearranging gives us

$$\left(\frac{\mathrm{d}u}{\mathrm{d}\phi}\right)^2 = \frac{E^2 + 2L}{\ell^2} - u^2 + 2Mu^3 - \frac{4ML}{\ell^2}u. \tag{2.16}$$

This equation determines the geometry of the geodesics and we will use 2.16 to search for an exact solution in terms of Jacobi elliptical functions. We can now differentiate 2.16 with respect to ϕ to give a more workable second order differential equation,

$$\frac{\mathrm{d}^2u}{\mathrm{d}\phi^2} + u = 3Mu^2 - \frac{2ML}{\ell^2}. \tag{2.17}$$

2.2 Exact Solutions to the Schwarzschild Metric

2.2.1 Time-Like Geodesics - Bound Orbits

Firstly we will consider bound orbits of a time-like particle. These occur when $E^2 < 1$ and $L = -\frac{1}{2}$. A bound orbit is one which has always been in the gravitational field of a mass, and without outside influence cannot escape its attraction. To search for an exact solution we use information provided by [4] and rewrite 2.16 as

$$\left(\frac{\mathrm{d}u}{\mathrm{d}\phi}\right)^2 = f(u) \tag{2.18}$$

where

$$\begin{aligned} f(u) &= 2Mu^3 - u^2 + \frac{2M}{\ell^2}u + \frac{E^2 - 1}{\ell^2} \\ &= 2M(u - u_1)(u - u_2)(u - u_3) \end{aligned} \tag{2.19}$$

Where u_1, u_2, u_3 are the solutions to the cubic equation, with $u_1 < u_2 < u_3$. If these are real we can write,

$$\begin{aligned} u_1 + u_2 + u_3 &= \frac{1}{2M}, \\ u_1u_2u_3 &= \frac{(1 - E^2)}{2M\ell^2}, \\ u_1u_2 + u_1u_3 + u_2u_3 &= \frac{1}{\ell^2}. \end{aligned} \tag{2.20}$$

At perihelion we have $\mathrm{d}u/\mathrm{d}\phi = 0$, therefore $f(u) = 0$. We can see from 2.19 that $f(u) > 0$ thus all roots are real, with $u_2, u_3 > 0$ and u_2 corresponds to the value at perihelion. There

is a possibility for two of the roots to be a complex conjugate pair, but we shall not be considering that particular case in this report.

We will now consider orbits of the first and second kind for distinct, real values of $0 < u_1 \leq u_2 \leq u_3$. We are interested in case where all three roots are distinct, however these conditions allow for cases with repeated roots which we will examine closer later. Orbits of the first kind exist when $u_1 \leq u \leq u_2$, ie an orbit which oscillates between to values of $r_1 = u_1^{-1}$ and $r_2 = u_2^{-1}$. Orbits of the second kind occur for $u \geq u_3$, ie an orbit which starts at an aphelion position $r_3 = u_3^{-1}$ and plummets into the singularity at $r = 0$.

We shall now write the three roots as

$$\begin{aligned} u_1 &= \frac{1}{l}(1-\epsilon) \\ u_2 &= \frac{1}{l}(1+\epsilon) \\ u_3 &= \frac{1}{2M} - \frac{2}{l}, \end{aligned} \tag{2.21}$$

where l is a positive constant known as the latus rectum, eccentricity exists in the range $0 \leq \epsilon < 1$ and u_3 is assigned as so to fulfil the conditions of 2.21.
It is important to note that due to the ordering of $0 < u_1 < u_2 < u_3$ we require

$$\frac{1}{2M} - \frac{2}{l} \geq \frac{1}{l}(1+\epsilon) \quad \text{or} \quad l \geq 2M(3+\epsilon). \tag{2.22}$$

Now we define $\mu = M/l$ to get the inequality

$$\mu \leq \frac{1}{2(3+\epsilon)} \quad \text{or} \quad 1 - 6\mu - 2\mu\epsilon \geq 0 \tag{2.23}$$

If we compare

$$f(u) = 2M(u - \frac{1}{l}(1-\epsilon))(u - \frac{1}{l}(1+\epsilon))(u - \frac{1}{2M} - \frac{2}{l}) \tag{2.24}$$

with 2.20, we get the relations

$$\frac{M}{\ell^2} = \frac{1}{l^2}[l - M(3+\epsilon^2)] \quad \text{and} \quad \frac{1-E^2}{\ell^2} = \frac{1}{l^3}(l-4M)(1-\epsilon^2). \tag{2.25}$$

We can rewrite these in terms of μ giving,

$$\frac{1}{\ell^2} = \frac{1}{lM}[1 - \mu(3+\epsilon^2)] \quad \text{and} \quad \frac{1-E^2}{\ell^2} = \frac{1}{l^2}(1-4\mu)(1-\epsilon^2) \tag{2.26}$$

Looking at the relations we can see that

$$\mu < (3+\epsilon^2)^{-1} \quad \text{and} \quad \mu < \frac{1}{4}. \tag{2.27}$$

We are now able to make the substitution

$$u = \frac{1}{l}(1 + \epsilon\cos\chi), \tag{2.28}$$

where χ is a new variable known as the relativistic anomaly. We can see that at aphelion $\chi = \pi$ and at perihelion $\chi = 0$.

Now upon substitution of 2.28 into 2.19 we find

$$\left(\frac{\mathrm{d}\chi}{\mathrm{d}\phi}\right)^2 = [(1 - 6\mu + 2\mu\epsilon) - 4\mu\epsilon\cos^2(\frac{1}{2}\chi)] \tag{2.29}$$

We can rewrite this as

$$\pm\frac{\mathrm{d}\chi}{\mathrm{d}\phi} = (1 - 6\mu + 2\mu\epsilon)^{\frac{1}{2}}(1 - k^2 cos^2(\frac{1}{2}\chi)) \tag{2.30}$$

where

$$k^2 = \frac{4\mu\epsilon}{1 - 6\mu + 2\mu\epsilon}. \tag{2.31}$$

From 2.24 we can see that

$$k^2 \leq 1 \quad \text{and} \quad 1 - 6\mu + 2\mu\epsilon > 0. \tag{2.32}$$

Due to this we can write the solution for ϕ in terms of the Jacobi elliptic integral

$$F(\psi, k) = \int_0^{\psi} \frac{1}{\sqrt{(1 - k^2\sin^2 y)}} dy \tag{2.33}$$

where $\psi = \frac{1}{2}(\pi - \chi)$. Therefore we can write

$$\phi = \frac{2}{(1 - 6\mu + 2\mu\epsilon)^{\frac{1}{2}}} F(\frac{1}{2}\pi - \frac{1}{2}\chi, k) \tag{2.34}$$

where the origin of ϕ is at aphelion where $\chi = \pi$.

Now we shall look at orbits of the second kind. As previously stated these orbits have their aphelion at u_3^{-1} and procede to the singularity at $r = 0$. We need to note that since $u_1 + u_2 + u_3 = 1/2M$ and $u_1 + u_2 > 0$ then $u_3 > 1/2M$, meaning that all these orbits start outside the event horizon. To obtain these orbits we firstly make the substitution

$$u = \left(\frac{1}{2M} - \frac{2}{l}\right) + \left(\frac{1}{2M} - \frac{3 + \epsilon}{l}\right)\tan^2(\frac{1}{2}\xi) \tag{2.35}$$

where previously we used 2.28. We can see that

$$\begin{gathered} u = u_3 = \frac{1}{2M} - \frac{2}{l} \quad \text{when} \quad \xi = 0 \\ \text{and} \\ u \to \infty \quad \text{as} \quad \xi \to \pi. \end{gathered} \tag{2.36}$$

Substitution of 2.36 into 2.19 gives

$$\left(\frac{\mathrm{d}\xi}{\mathrm{d}\phi}\right)^2 = (1 - 6\mu + 2\mu\epsilon)(1 - k^2\sin^2(\frac{1}{2}\xi)) \tag{2.37}$$

where k^2 has the same definition as for orbits of the first kind. Again this solution can be expressed using the Jacobi elliptic function we saw in 2.33 . Thus we can write

$$\phi = \frac{2}{(1 - 6\mu + 2\mu\epsilon)^{\frac{1}{2}}} F(\frac{1}{2}\xi, k). \tag{2.38}$$

We can see an example of this orbit iin Figure 2.1.

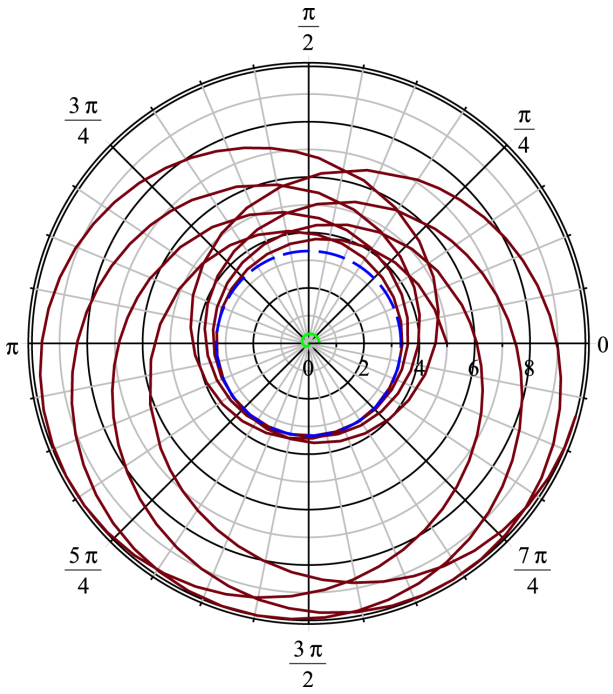

Figure 2.1: A bound orbit with $l = 5$, $\epsilon = 1/2$ and $M = 1/6$. The red line shows the orbit of the first kind, which does a large orbit of the black hole from its aphelion distance, followed by a smaller orbit where it achieves its perihelion distance, at $r = 10$ and $r = 10/3$ respectively. The green line shows the orbit of the second kind which plummets into the black hole from its aphelion distance of $r = 5/13$. The blue line indicates the perihelion distance at $r = 3$. Distances have been scaled in terms of the Schwarzschild radius.

2.2.2 Time-Like Geodesics - Special Cases of Bound Orbits

We will now consider two special cases for the time-like geodesics, as demonstrated in [5]. The first case, (a), is when $\epsilon = 0$. This leads to a circular orbit of the first kind with constant radius $r_c = l$ and an orbit of the second kind plunging into the singularity.

The second case, (b), is when $2\mu(3 + \epsilon) = 1$ which leads to the orbit asymptotically approaching its perihelion distance r_2 and circling around it an infinite number of times before evenutally the orbit of the second kind plunges into the singularity.

Case (a): Firstly we will search for orbits of the first kind. Setting $\epsilon = 0$ we find that we have a repeated root, $u_1 = u_2 = u_c$, which gives us a critical radius at $r_c = l$ and we see $\mu = M/r_c$. We must now rewrite our equations for angular momentum and energy as,

$$\frac{1}{\ell^2} = \frac{1 - 3M/r_c}{r_c M} \quad \text{and} \quad \frac{E^2}{\ell^2} = \frac{(2M/r_c - 1)^2}{r_c M}. \tag{2.39}$$

If we now rewrite the first equation as

$$r_c^2 - \frac{\ell^2}{M} r_c + 3\ell^2 = 0 \tag{2.40}$$

we see that an orbit with zero eccentricity must have one of the two roots,

$$r_c = \frac{\ell^2}{2M}\left[1 \pm \left(1 - 12M^2/\ell^2\right)^{\frac{1}{2}}\right], \tag{2.41}$$

and that no circular orbits is possible if

$$\frac{\ell}{M} < 2\sqrt{3}. \tag{2.42}$$

We now take the minimum allowed value of $\ell/M = 2\sqrt{3}$ and see that,

$$r_c = 6M \quad \text{and} \quad E^2 = \frac{8}{9}. \tag{2.43}$$

This value of r_c is the largest unstable orbit. Smaller values for ℓ/M give us larger values for r_c, in the region $6M < r_c < \infty$, which results in a stable orbits. Orbits provided by $\ell/M > 2\sqrt{3}$ result in unstable orbits in the region $3M \leq r_c \leq 6M$.

Now we will search for orbits of the second kind. From 2.31 we can see that $k = 0$ when $\epsilon = 0$, therefore we integrate 2.29 to find

$$\chi = (1 - 6\mu)^{1/2}(\phi - \phi_0), \tag{2.44}$$

where ϕ_0 is a constant of integration. Substituting this into 2.35 we find that our solution takes the form

$$u = \frac{1}{l} + \left(\frac{1}{2M} - \frac{3}{l}\right) \sec^2\left[\frac{1}{2}(1 - 6\mu)^{1/2}(\phi - \phi_0)\right]. \tag{2.45}$$

Despite ϵ being zero, this orbit of the second kind is not a circle! It starts at aphelion in the range $3M \leq r_3 \leq 6M$ where $\phi = \phi_0$, and arrives at the singuarity, $r = 0$, when

$$\phi - \phi_0 = \pi/(1 - 6\mu)^{1/2}. \tag{2.46}$$

We can see an example of this orbit in Figure 2.2.

We can see from 2.44 we must consider the case when $\epsilon = 0$ and $\mu = 1/6$. In this case all three roots of $f(u) = 0$ coincide and $u_1 = u_2 = 1/6M$. We now write 2.19 as

$$\left(\frac{\mathrm{d}u}{\mathrm{d}\phi}\right)^2 = 2M\left(1 - \frac{1}{6M}\right)^3, \tag{2.47}$$

which can be solved to give a solution as

$$u = \frac{1}{6M} + \frac{2}{M(\phi - \phi_0^2)}. \tag{2.48}$$

We can see an example of this orbit in Figure 2.3.

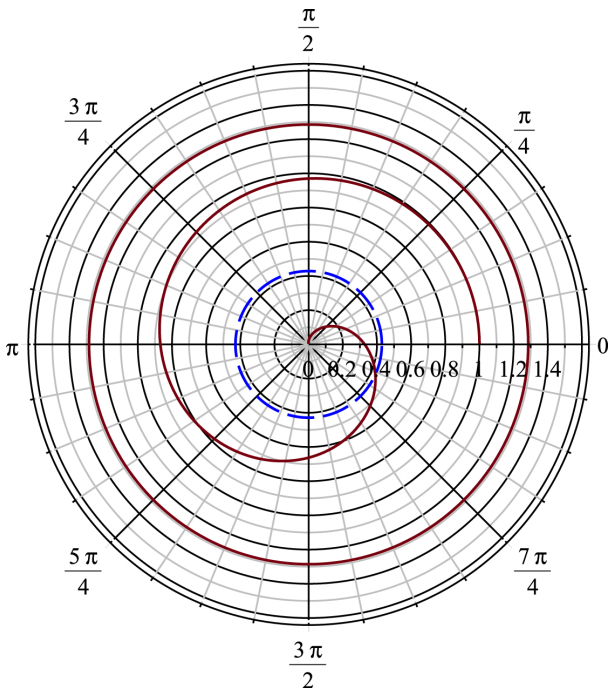

Figure 2.2: A bound orbit with $l = 3/2$, $\epsilon = 0$ and $M = 3/14$. The circular red line shows the orbit of the first kind, which orbits the black hole an infinite number of times from a distance $r_c = 9/7$. The spiralling red line shows the orbit of the second kind which plummets into the black hole from its aphelion distance of $r \approx 1$. The dashed blue line indicates the event horizon at a distance $r_s = 3/7$. Distances have been scaled in terms of the Schwarzschild radius.

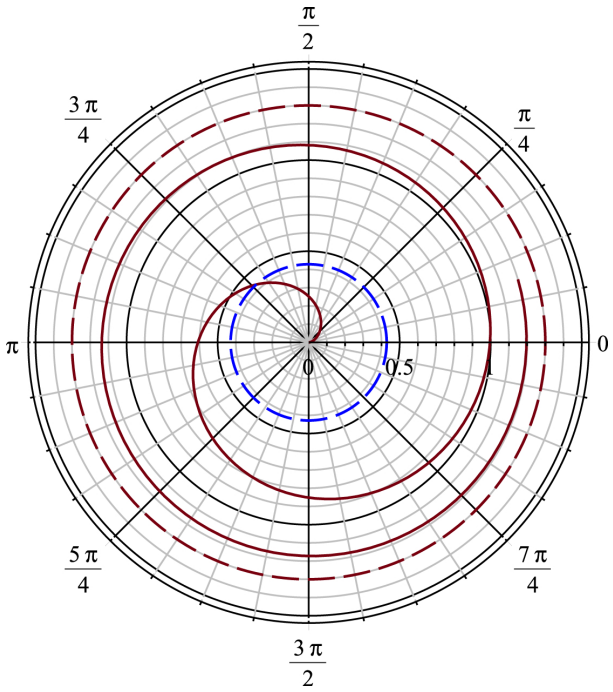

Figure 2.3: A bound orbit with $\mu = 1/6$, $\epsilon = 0$ and $M = 3/14$. The dashed circular red line shows the smallest stable orbit at a distance $r_c = 9/7$. The spiralling red line shows the orbit of the second kind which plummets into the black hole from its stable orbit. The dashed blue line indicates the event horizon at a distance $r_s = 3/7$. This plot is very similar to figure 2.2, with the difference that the direction of the orbit is reversed. Distances have been scaled in terms of the Schwarzschild radius.

Case (b): Again, we will initially search for orbits of the first kind. In this case we have the repeated root at $u_2 = u_3$. Substituting $2\mu(3+\epsilon) = 1$ into 2.21 we find

$$r_2 = \frac{l}{1+\epsilon} = 2M\frac{3+\epsilon}{1+\epsilon} \quad \text{and} \quad r_1 = 2M\frac{3+\epsilon}{1-\epsilon}, \tag{2.49}$$

where r_1 and r_2 are, respectively, our perihelion and aphelion distances. From this it follows that the range for perihelion is restricted to

$$4M \leq r_2 < 6M. \tag{2.50}$$

Using 2.26 we find the relations

$$\frac{\ell^2}{M^2} = 4\frac{(3+\epsilon)^2}{(3-\epsilon)(1+\epsilon)} \quad \text{and} \quad 1 - E^2 = \frac{1-\epsilon^2}{9-\epsilon^2}. \tag{2.51}$$

The elliptic modulus, k, becomes 1 and we therefore return to 2.29 to find

$$\left(\frac{\mathrm{d}\chi}{\mathrm{d}\phi}\right)^2 = 4\mu\epsilon\sin^2(\frac{1}{2}\chi), \tag{2.52}$$

which can be written as

$$\frac{\mathrm{d}\chi}{\mathrm{d}\phi} = -2(\mu\epsilon)^{\frac{1}{2}}\sin(\frac{1}{2}\chi), \tag{2.53}$$

where we chose the negative sign so that ϕ increases when χ decreases from its aphelion value π. We now integrate 2.53 to give the solution

$$\phi = -\frac{1}{\sqrt{\mu\epsilon}}\ln\left[\tan\left(\frac{1}{4}\chi\right)\right]. \tag{2.54}$$

We see that $\phi \to \infty$ when $\chi \to 0$. This shows that as perihelion is approached the orbit spirals around the circle at r_2 an inifinte number of times.

We will now search for the orbit of the second kind. We cannot obtain this solution by simply setting $\mu = 1/2(3+\epsilon)$ in 2.37 as the coefficient $\tan^2(\chi/2)$ vanishes. We must consider this case from the very beginning. Firstly we note that when $2\mu(3+\epsilon) = 1$ our three roots are

$$u_1 = \frac{1-\epsilon}{l} \quad \text{and} \quad u_2 = u_3 = \frac{1+\epsilon}{l}, \tag{2.55}$$

and the substitution suggested is

$$u = \frac{1}{l}\left[1 + \epsilon + 2\epsilon\tan^2\left(\frac{1}{4}\xi\right)\right]. \tag{2.56}$$

We can see that, by this substitution,

$$u = u_2 = u_3 = \frac{1+\epsilon}{l} \quad \text{when} \quad \xi = 0, \quad \text{and} \quad u \to \infty \quad \text{when} \quad \xi = \pi. \tag{2.57}$$

Using our substitution from 2.56 in 2.19 gives

$$\left(\frac{\mathrm{d}\chi}{\mathrm{d}\phi}\right)^2 = 4\mu\epsilon\sin^2(\frac{1}{2}\chi) \tag{2.58}$$

which is the exact same solution as for orbits of the first kind. We therefore write our solution as

$$\phi = -\frac{1}{\sqrt{\mu\epsilon}} \ln\left[\tan\left(\frac{1}{4}\chi\right)\right]. \tag{2.59}$$

We see that, $\phi = 0$ when $\xi = \pi$ and $r \to 0$; and $\phi \to \infty$ as $\xi \to 0$ and aphelion is approached at $r = l/(1+\epsilon)$. This means the orbit approaches the aphelion by spiralling around it an infinite number of times. This is the same orbits of the first kind, only their perihelion is now the aphelion for orbits of the second kind. We can see an example of this orbit in Figure 2.4.

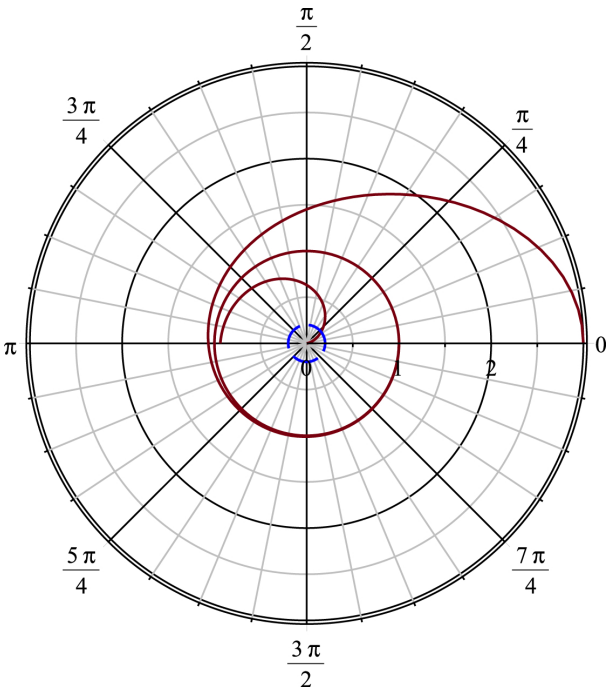

Figure 2.4: A bound orbit with $\mu = 3/2$, $\epsilon = 1/2$ and $M = 3/14$. The orbit of the first kind approaches the circle at its perihelion distance, $r = 1$, asymptotically and spirals around it an infinite number of times. The orbit of the second kind then spirals into the singularity after spiralling around. The red line shows the orbit of the second kind which plummets into the black hole from $r = 1$. The dashed blue line indicates the event horizon at a distance $r_s = 3/7$. Distances have been scaled in terms of the Schwarzschild radius.

2.2.3 Time-Like Geodesics - Unbound Orbits

Now we will consider unbound orbits of a time-like particle, as done by [6]. These occur when $E^2 > 1$ and $L = -1/2$. If $E^2 > 1$ we find that the term $(E^2 - 1)/\ell^2$ is constant, indicating that the equation $f(u) = 0$ must allow a negative root. In this case we will take $u_1 < 0$, $u_2, u_3 > 0$ and $u_1 < 0 < u_2 < u_3$. As all three roots are real and two of them are positive, we must again distinguish between orbits of the first and second kind. We find that orbits of the first kind are restricted to $0 < u \leq u_2$ and orbits of the second kind are restricted to $u \geq u_3$. Similar to bound orbits there is a possibility of imaginary roots, which we will not be considering in this report.

Once again we will shall continue to express the roots in terms of an eccentricity ϵ , with the difference from bound orbits being that $\epsilon \geq 1$. Therefore we may write

$$u_1 = -\frac{1}{l}(\epsilon - 1), \qquad u_2 = \frac{1}{l}(\epsilon + 1) \qquad \text{and} \qquad u_3 = \frac{1}{2M} - \frac{2}{l}. \tag{2.60}$$

The inequality,

$$1 - 6\mu - 2\mu\epsilon > 0, \tag{2.61}$$

still applies, as it is assumed only wih regards to the ordering of the roots: $u_1 < u_2 < u_3$. We can see that the relations 2.26 continue to hold, with the exception that $\epsilon \geq 1$. We may therefore write,

$$\frac{1}{\ell^2} = \frac{1}{lM}[1 - \mu(3 + \epsilon^2)] \qquad \text{and} \qquad \frac{E^2 - 1}{\ell^2} = \frac{1}{l^2}(1 - 4\mu)(\epsilon^2 - 1). \tag{2.62}$$

Since $\ell^2 > 0$ and $E^2 - 1 \geq 0$ we can see,

$$1 - \mu(3 + \epsilon^2) > 0 \quad \text{and} \quad \mu \leq \frac{1}{4}. \tag{2.63}$$

As before we shall now use the substitution,

$$u = \frac{1}{l}(1 + \epsilon \cos\chi). \tag{2.64}$$

However, since $\epsilon \geq 1$ we find,

$$u = 0 \quad \text{when} \quad \chi = \cos^{-1}(-\epsilon^{-1}) = \chi_\infty. \tag{2.65}$$

Despite of that, the perihelion passage still occurs at $\chi = 0$. We therefore find the range of χ to be,

$$0 \leq \chi < \chi_\infty = \cos^{-1}(-\epsilon^{-1}). \tag{2.66}$$

Despite these restrictions on the range of χ, our solution takes a form similar to that found in the previous section. Once again using Jacobi elliptic functions with the same elliptic modulus, k. Thus we find a solution for ϕ in the form,

$$\phi = \frac{2}{(1 - 6\mu + 2\mu\epsilon)^{\frac{1}{2}}}\left[K(k) - F(\frac{1}{2}\pi - \frac{1}{2}\chi, k)\right], \tag{2.67}$$

where $K(k)$ denotes the complete elliptic integral,

$$K(k) = \int_0^{\frac{\pi}{2}} \frac{1}{\sqrt{(1 - k^2 \sin^2 y)}} dy. \tag{2.68}$$

We can see an example of this orbit in Figure 2.5.

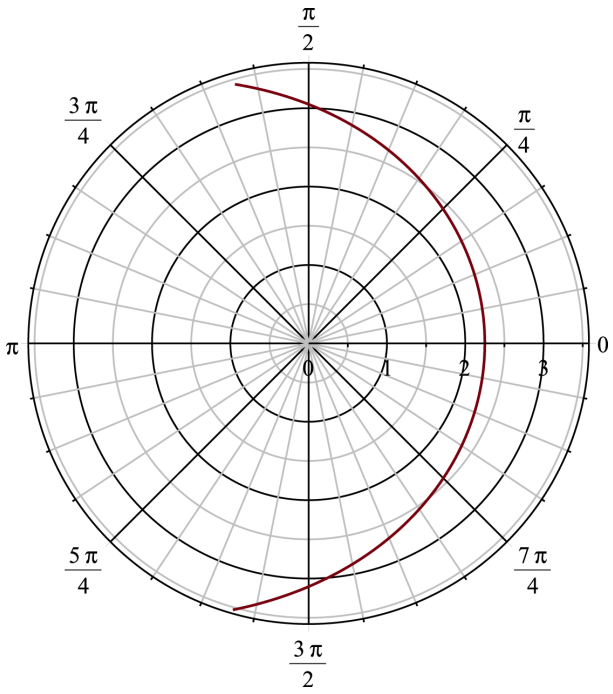

Figure 2.5: A unbound orbit for a time-likel geodesic with $l = 5/2$, $e = 3/2$ and $M = 3/14$. The test particle comes in from infinity towards the black hole, it is then bent around it and continues to infinity in the opposite direction to which it approached. Distances have been scaled in terms of the Schwarzschild radius.

2.2.4 Null Geodesics - Bound Orbits

We saw earlier that for a particle which has zero rest mass, ie light, we must set the Lagrangian in 2.7 equal to zero. Using [7] we our Lagrangian becomes,

$$\begin{aligned} 0 &= -\frac{E^2}{2F(r)} + \frac{\dot{r}^2}{2F(r)} + \frac{\ell^2}{2r^2}, \\ &= \frac{E^2}{1-2M/r} - \frac{\dot{r}^2}{1-2M/r} - \frac{\ell^2}{r^2}. \end{aligned} \tag{2.69}$$

Working through as before we can rewrite 2.69 as,

$$\left(\frac{\mathrm{d}u}{\mathrm{d}\phi}\right)^2 = 2Mu^3 - u^2 + \frac{1}{D^2} = f(u), \tag{2.70}$$

where $D = \ell/E$ denotes the impact parameter. This is defined as the perpendicular distance between the path of an object and the center of the gravitational field created by the object which the object is orbiting.

Once again we assume that all roots are real we get the relations,

$$\begin{aligned} u_1 + u_2 + u_3 &= \frac{1}{2M} \\ u_1 u_2 u_3 &= -\frac{1}{2MD^2} \end{aligned} \tag{2.71}$$

We can clearly see that $f(u) = 0$ must allow for a negative root, with the two remaining roots being either real or a complex conjugate pair. This case is true for both the bound

and unbound orbits. However, the bound where the two positive real roots correspond results in a special case, which are known as the critical orbits.

Examining the derivative of 2.70,

$$6Mu^2 - 2u = f'(u) = 0, \tag{2.72}$$

gives us a critical root of $u = 1/3M$. Upon subtitution back into 2.70 we can see that this root occurs if $D^2 = 27M^2$. Using the conditions we have previously set, we can see that the three roots of 2.70 are,

$$u_1 = -\frac{1}{6M}, \qquad u_2 = u_3 = \frac{1}{3M} \quad \text{and} \quad D = (3\sqrt{3})M. \tag{2.73}$$

We can see that because $du/d\phi$ vanishes for $u = 1/3M$ and $D = (3\sqrt{3})M$, non-stable circular orbits of radius $3M$ are allowed.

To better get a grasp of the orbits, we will now consider the full equation for this case,

$$\left(\frac{\mathrm{d}u}{\mathrm{d}\phi}\right)^2 = 2M\left(u + \frac{1}{6M}\right)\left(u - \frac{1}{3M}\right)^2. \tag{2.74}$$

To find the orbits of the first kind for null geodesics we note that the above equation is satisfied by the following substitution, as seen in [7] ,

$$u = \frac{1}{6M} + \frac{1}{2M}\tanh^2(\frac{1}{2}(\phi - \phi_0)), \tag{2.75}$$

where ϕ_0 is a constant of integration. If we choose this constant to be

$$\tanh^2(\frac{1}{2}\phi_0) = \frac{1}{3}, \tag{2.76}$$

then we see

$$u = 0 \quad \text{and} \quad r \to \infty \quad \text{when} \quad \phi = 0. \tag{2.77}$$

However we also see that,

$$u = \frac{1}{3M} \quad \text{when} \quad \phi \to \infty. \tag{2.78}$$

This tells us that for a particle with zero rest mass approaching from infinity, with impact parameter as specified, advances asymptotically towards a circle of radius $3M$, by spiralling around it.

Now we shall search for a solution for orbits of the second kind, which orbit around $r = 3M$ before diving into the singularity. To find these solutions we must again use a subsitution in equation 2.70,

$$u = \frac{1}{3M} + \frac{1}{2M}\tan^2(\frac{1}{2}\xi). \tag{2.79}$$

Upon rearrangement we reduce the equation to

$$\left(\frac{\mathrm{d}\xi}{\mathrm{d}\phi}\right)^2 = \sin^2(\frac{1}{2}\xi). \tag{2.80}$$

Taking the square root and integrating gives us,

$$\begin{aligned}\int \frac{1}{\sin(\frac{1}{2}\xi)} &= 2\ln\left(\sin\left(\frac{\xi}{4}\right)\right) - 2\ln\left(\cos\left(\frac{\xi}{4}\right)\right) \\ &= 2\ln\left(\tan\left(\frac{\xi}{4}\right)\right),\end{aligned} \tag{2.81}$$

which can be rearranged to give

$$\xi = 4\arctan(e^{(\frac{\phi}{2})}). \tag{2.82}$$

Substituting 2.82 into 2.79 and rearranging using the trigonometric identity $\tan(2\theta) = 2\tan(\theta)/(1-\tan^2(\theta))$ we obtain,

$$u = \frac{1}{3M} + \frac{2e^{\phi}}{M(e^{\phi}-1)^2}. \tag{2.83}$$

We can see that for this orbit,

$$u \to \infty \quad \text{and} \quad r \to 0 \quad \text{when} \quad \phi \to 0 \tag{2.84}$$

and

$$u \to \frac{1}{3M} \quad \text{as} \quad \phi \to \infty, \tag{2.85}$$

provided the attributes stated in 2.73 are applied. We may consider the solution in 2.83, with the sign reversed, as a continuation of 2.75. We show an example of this orbit in Figure 2.6.

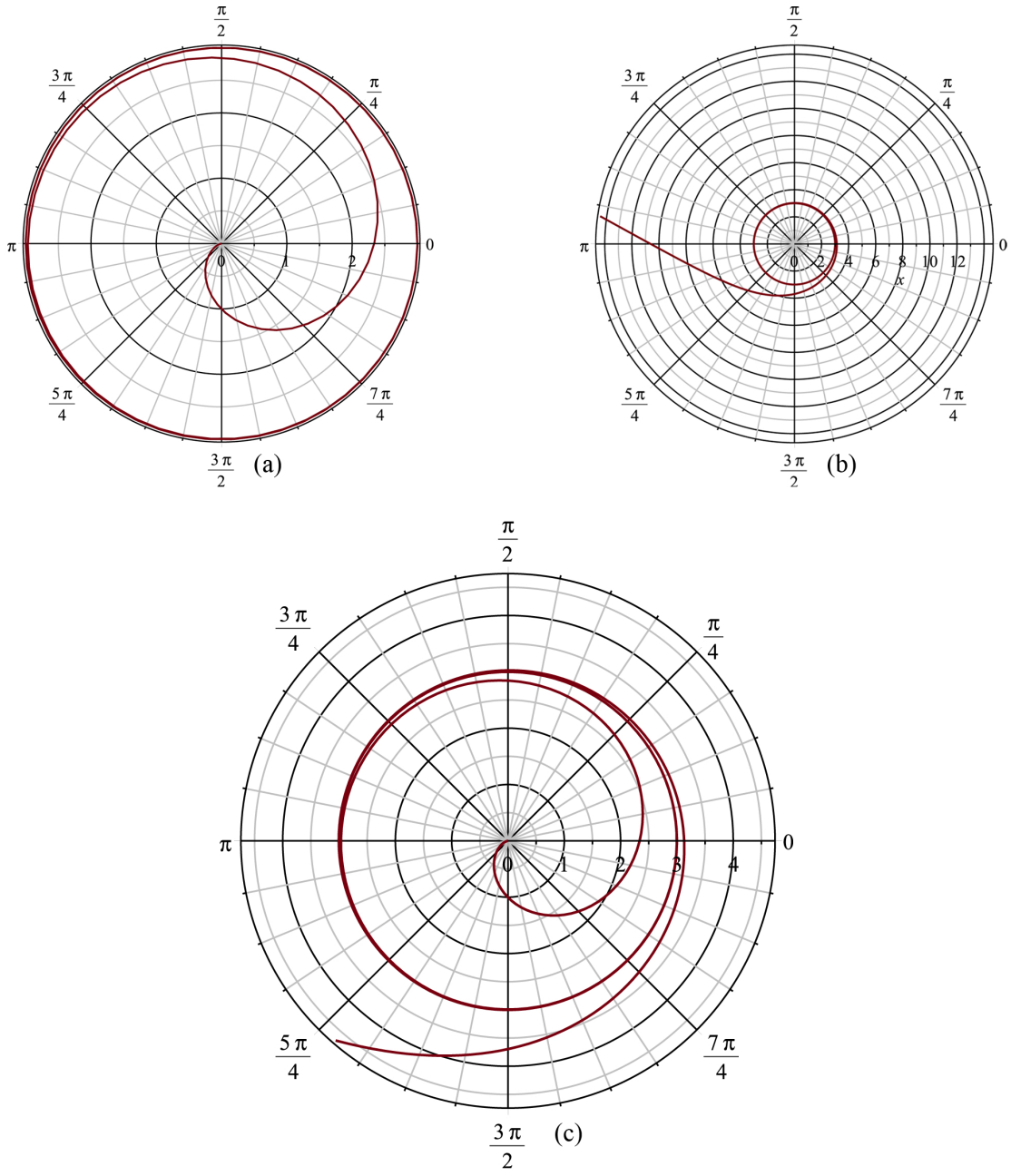

Figure 2.6: All figures (a),(b) and (c) use the roots specified in 2.73, as well as the mass $M = 1$. (a) shows the bound orbit of the first kind for a test particle, which comes in from infinity and ends up spiralling around the critial radius $r = 3M$. (b) shows the bound orbit of the second kind for a test particle, which starts orbiting the black hole at radius $r = 3M$ before eventually plunging into the singularity. It is important to note that in (b) the sign of 2.83 has been reversed as to indicate a particle moving towards the singularity, not away from it. (c) shows the combined effect of test particle which initially approaches from infinity, circles around the unstable orbit of the black hole at radius $r = 3M$, eventually passes the event horizon and spiralls to the singularity. It is interesting to note that the direction of motion for (b) is opposite to that of (a). Distances have been scaled in terms of the Schwarzschild radius.

2.2.5 Null Geodesics - Unbound Orbits

As for the bound orbits of null geodesics the Lagrangian must be equal to zero. However, we will now consider the the case where all three roots of $f(u) = 0$ are real and the two positive roots are distinct. In this case we will take $u_1 < 0$, $u_2, u_3 > 0$ and $u_1 < u_2 < u_3$.

Using [8] we shall now define the roots as,

$$u_1 = \frac{P - 2M - Q}{4MP}, \quad u_2 = \frac{1}{P} \quad \text{and} \quad u_3 = \frac{P - 2M + Q}{4MP}. \tag{2.86}$$

P denotes the perihelion distance and Q is a constant which will be identified shortly. Note that the sums of these roots is $1/2M$ and the ordering requires

$$Q + P - 6M > 0. \tag{2.87}$$

Next, we use

$$f(u) = 2M(u - u_1)(u - u_2)(u - u_3), \tag{2.88}$$

with the three roots defined as above, to obtain

$$Q^2 = (P - 2M)(P + 6M) \quad \text{and} \quad \frac{1}{D^2} = \frac{1}{8MP^3}(Q^2 - (P - 2M)^2). \tag{2.89}$$

Combining these two relations helps simplify the second, giving

$$D^2 = \frac{P^3}{P - 2M}. \tag{2.90}$$

We may also combine 2.87 and 2.89 to give

$$(P - 2M)(P + 6M) > (P - 6M)^2, \tag{2.91}$$

which simplifies to,

$$P > 3M. \tag{2.92}$$

From 2.90 we can obtain the inequality

$$D > (3\sqrt{3})M = D_c \tag{2.93}$$

This means that we are only now considering orbits which have the impact parameter above the critical value and are entirely outside of the circle $r = 2M$.

To start searching for orbits of the first kind we we make the substitution, provided by chandresakhar,

$$u - \frac{1}{P} = -\frac{Q - P + 6M}{8MP}(1 + \cos\chi), \tag{2.94}$$

from which it follows that

$$u + \frac{Q - P + 2M}{4MP} = \frac{Q - P + 6M}{8MP}(1 - \cos\chi). \tag{2.95}$$

By this substitution,

$$\begin{aligned} u = \frac{1}{P} \quad &\text{when} \quad \chi = \pi \\ &\text{and} \\ u = 0 \ \text{ and } \ r \to \infty \ &\text{when} \ \ \sin^2(\frac{1}{2}\chi) = \frac{Q - P + 2M}{Q - P + 6M} = \sin^2(\frac{1}{2}\chi_\infty) \end{aligned} \tag{2.96}$$

Substitution of 2.94 and 2.95 into 2.70 gives

$$\left(\frac{\mathrm{d}\chi}{\mathrm{d}\phi}\right)^2 = \frac{Q}{P}(1 - k^2 \sin^2(\frac{1}{2}\chi)), \tag{2.97}$$

where

$$k^2 = \frac{1}{2Q}(Q - P + 6M). \tag{2.98}$$

Once again we can express a solution for ϕ in terms of Jacobi elliptic functions,

$$\phi = 2\left(\frac{P}{Q}\right)^{\frac{1}{2}}[K(k) - F(\frac{1}{2}\chi, k)]. \tag{2.99}$$

Using the relations in 2.96 we can show the asymptotic value of ϕ as $r \to \infty$ is,

$$\phi_\infty = 2\left(\frac{P}{Q}\right)^{\frac{1}{2}}[K(k) - F(\frac{1}{2}\chi_\infty, k)]. \tag{2.100}$$

To search for orbits of the second kind we use another substitution, as done by [8],

$$u = \frac{1}{P} + \frac{Q + P - 6M}{4MP}\sec^2(\frac{1}{2}\chi). \tag{2.101}$$

We repeat the previous process done for 2.94. We can see that,

$$u \ \text{ is at aphelion when } \quad u = u_3 = \frac{1}{4MP}(Q + P - 2M) \quad \text{and} \quad \chi = 0, \tag{2.102}$$

and

$$u \to \infty \quad \text{and} \quad r \to 0 \quad \text{when} \quad \chi = \pi. \tag{2.103}$$

Substitution 2.101 reduces to the same form as 2.97, with the same value of k^2. Thus we may write our solution as

$$\phi = 2\left(\frac{P}{Q}\right)^{\frac{1}{2}}[F(\frac{1}{2}\chi, k)], \tag{2.104}$$

where the origin of the particle is at aphelion. We can see an example of this orbit in Figure 2.7.

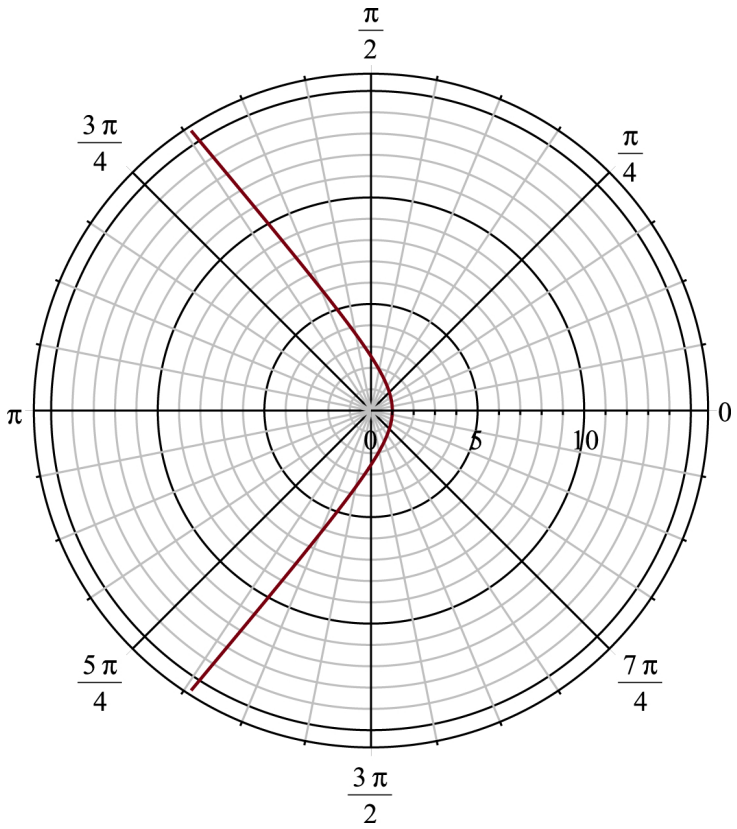

Figure 2.7: A unbound orbit for a null geodesic with $P = 1$, $Q \approx 0.76$ and $M = 3/14$. The test particle comes in from infinity towards the black hole in a straight line, it is then bent around it and continues straight to infinity in the opposite direction to which it approached. We notice that this orbit is very similar to that seen in figure 2.5 for unbound time-like particles, however as these are null geodesics the orbit is straight when it does not feel the immediate effects of the black hole. Distances have been scaled in terms of the Schwarzschild radius.

Chapter 3

Approximate Solutions and Perihelion Precession

3.1 Schwarzschild Solution

In this section we will consider how a planet precesses around our sun with regards to Einstein's theory of General Relativity. This is possible as, to a decent approximation, the sun can be considered to be spherical, meaning that Schwarzschild geometry will give an effective approximate solution. We have already seen that the Schwarzschild solution can be solved exactly, however approximate methods are a powerful tool which can be used for more advanced metrics, therefore I have included the approximate solution for Schwarzschild to demonstrate this, as seen in [9].

As we are dealing with massive planets we take $L = -\frac{1}{2}$ in 2.17, giving us

$$\frac{\mathrm{d}^2 u}{\mathrm{d}\phi^2} + u = \frac{3M^2}{u} + \frac{ML}{\ell^2}. \tag{3.1}$$

From observsational evidence it is clear that the motion of the closest planets are near to being circular. We know that a circular orbit has constant radius, so for our case we want to set our radius to have a slight correction due to general relativity. We will take

$$u = \frac{M}{\ell^2}\left[1 + \epsilon f\left(\phi\right)\right] \tag{3.2}$$

for a function $f(\phi)$ and constant eccentricity ϵ. Due to our orbit being almost circular we require $|\epsilon f(\phi)| \ll 1$. Substituting 3.2 into 3.1, and cancelling down, gives

$$f'' + \left(1 - \frac{6M^2}{\ell^2}\right) f = \frac{3M^2}{\ell^2 \epsilon} \tag{3.3}$$

Now if we let $\omega^2 = 1 - 6M^2/\ell^2$ we can see that

$$f(\phi) \propto \cos(\omega\phi) \tag{3.4}$$

Now we consider an elliptical orbit in Newtonian physics; we call r_- the point of closest approach and r_+ the point of furthest approach. We can now define a semi-major axis a as

$$r_- + r_+ = 2a. \tag{3.5}$$

The eccentricity of an ellipse indicates how circular it is. If $\epsilon = 0$ then we have a circular orbit. We can now define eccentricity as

$$r_+ - r_- = 2a\epsilon. \tag{3.6}$$

From equation 3.2 we can see

$$\frac{1}{r_-} = \frac{M}{\ell^2}(1+\epsilon) \tag{3.7}$$

$$\frac{1}{r_+} = \frac{M}{\ell^2}(1-\epsilon) \tag{3.8}$$

and thus using 3.5 to 3.8 we deduce that

$$r_+ = a(1-\epsilon), \tag{3.9}$$

$$r_- = a(1+\epsilon), \tag{3.10}$$

$$\frac{M}{\ell^2} = \frac{1}{a(1-\epsilon^2)}. \tag{3.11}$$

Returning to general relativity we can see that $f(\phi) \propto \cos(\omega\phi)$ and not just $cos(\phi)$. This means the orbits are not periodical in 2π. From this we can find the change in ϕ per revolution.

$$\begin{aligned} \Delta\phi = \frac{2\pi}{\omega} - 2\pi &= 2\pi\left(1 - \frac{6M}{a(1-\varepsilon^2)}\right)^{-\frac{1}{2}} - 2\pi \\ &\approx 2\pi\left(1 + \frac{3M}{a(1-\varepsilon^2)}\right) - 2\pi \end{aligned} \tag{3.12}$$

If we use u_1 and u_2 from 2.21 along with 3.9 and 3.10, we can show

$$\frac{1}{l} = \frac{1}{2}\left(\frac{1}{r_1} + \frac{1}{r_2}\right) \tag{3.13}$$

and

$$\frac{1}{l} = \frac{1}{a\,(1-\epsilon^2)}. \tag{3.14}$$

Upon substitution of 3.14 into 3.12 we find

$$\Delta\phi = 6\pi\frac{M}{l} = 6\pi\frac{M}{a(1-\epsilon^2)}. \tag{3.15}$$

Using 3.14 our approximate solution now becomes

$$u = \frac{1}{l}\left[1 + \epsilon\cos(\omega\phi)\right] \tag{3.16}$$

We can see an example of this orbit in Figure 3.1.

We can use 3.15 to find the perihelion precession of the orbit shown in figure 2.3, where $l = 6$, $\epsilon = 1/2$ and $M = 1/6$. Therefore,

$$\Delta\phi = \frac{\pi}{6} = 30^\circ. \tag{3.17}$$

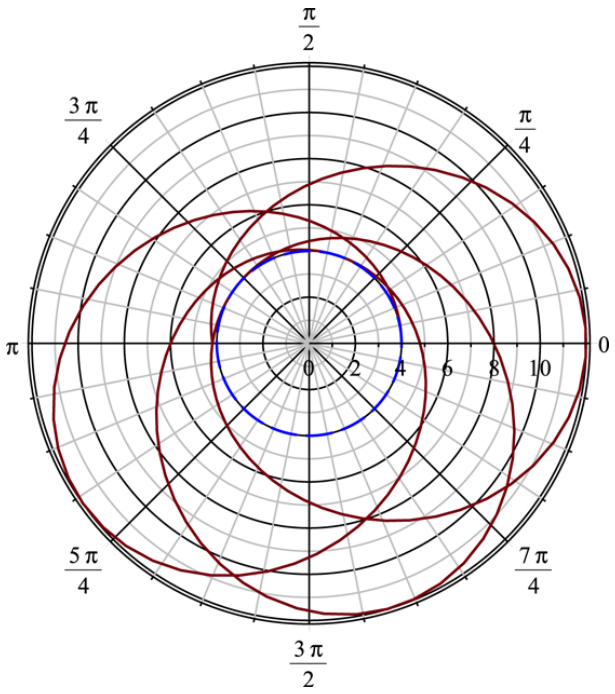

Figure 3.1: An approximate bound orbit with $l = 6$, $\epsilon = 1/2$ and $M = 1/6$. The red line indicates the orbit of a test particle with aphelion at $r = 12$ and perihelion at $r = 4$, with the latter indicated by the dashed blue line. Distances have been scaled in terms of the Schwarzschild radius.

3.2 de Sitter - Schwarzschild Metric

When Albert Einstein created his theory of general relativity he found it predicts that the universe must either expand or contract which differed from his view that it was static. This led to him introducing a constant which would halt this expansion, known as the cosmological constant, Λ. When Hubble discovered that the universe was indeed expanding, apparently proving that Einstein was wrong, Einstein called the cosmological constant his greatest mistake.

However, recent research into dark energy, a theorised form of energy which makes up $\approx 68\%$ of our universe and causes expansion, has been linked with the cosmological constant, suggesting that dark energy has a constant energy density throughout the universe. This happened in the 1990s when observational evidence from a supernova 7 billion light years away suggested that the expansion of the universe was slower than it is today. This surprised researchers as they believed the expansion of the universe was slowing down due to the effect of gravity, however the observational evidence suggested the opposite.

The cosmological constant was combined with the Friedmann-Lemaître-Robertson-Walker (FLRW) metric, which is is an exact solution of general relativity, to create the Lamda-CDM model which is commonly known as the *standard model* due to its simplicity and the precise accuracy with which it agrees with observations. However, in this section we will be considering a slightly modified version of the previously seen Schwarzschild

metric in 2.1, known as the de Sitter - Schwarzschild Metric. $F(r)$ now takes the form

$$F(r) = 1 - \frac{2M}{r} - \frac{\Lambda r^2}{3}, \tag{3.18}$$

where Λ is the cosmological constant. We will reuse the definitions for energy and angular momentum from 2.5 and 2.6. Our Lagrangian remains the same, thus we may use the substitutions 2.10 - 2.15 in 2.7, which retains the conditions described in 2.9. Upon substitution we find

$$\left(\frac{\mathrm{d}u}{\mathrm{d}\phi}\right)^2 = \frac{E^2 + 2L}{\ell^2} - u^2 + 2Mu^3 - \frac{4ML}{\ell^2}u + \frac{\Lambda}{3}\left(1 - \frac{2L}{\ell^2 u^2}\right). \tag{3.19}$$

We can now differentiate 3.19 with respect to ϕ, giving us

$$\frac{\mathrm{d}^2u}{\mathrm{d}\phi^2} + u = 3Mu^2 - \frac{2ML}{\ell^2} + \frac{2}{3\ell^2}\frac{\Lambda L}{u^3}. \tag{3.20}$$

We are now going to search for an approximate solution using a similar method to that in section 2.2. This will give us an idea of how much a large body precesses around a mass when there is a cosmological constant present. Taking $L = -1/2$ for a large bodies, we see that 3.20 takes the form

$$\frac{\mathrm{d}^2u}{\mathrm{d}\phi^2} + u = 3Mu^2 + \frac{M}{\ell^2} - \frac{1}{3\ell^2}\frac{\Lambda}{u^3}. \tag{3.21}$$

We may use the same assumption from 3.2,

$$u = \frac{M}{\ell^2}\left[1 + \epsilon f\left(\phi\right)\right]. \tag{3.22}$$

Substituting 3.2 into 3.21 gives

$$f'' + \left(1 - \frac{6M^2}{\ell^2} - \frac{\ell^6\Lambda}{M^4}\right) f = \frac{3M^2}{\ell^2\epsilon} - \frac{\ell^6\Lambda}{3M^4}. \tag{3.23}$$

We can see that due to the right hand side being constant, this gives us a solution in the form

$$f(\phi) \propto \cos(\omega\phi), \tag{3.24}$$

where

$$\omega^2 = 1 - \frac{6M^2}{\ell^2} - \frac{\ell^6\Lambda}{M^4}. \tag{3.25}$$

Using 3.5 to 3.11 we can see that

$$\begin{aligned} \Delta\phi = \frac{2\pi}{\omega} - 2\pi &= 2\pi\left(1 - \frac{6M}{a(1-\varepsilon^2)} - \frac{a^3\left(1-\epsilon^2\right)^3\Lambda}{M}\right)^{-\frac{1}{2}} - 2\pi, \\ &\approx 2\pi\left(1 + \frac{3M}{a(1-\varepsilon^2)} + \frac{a^3\left(1-\epsilon^2\right)^3\Lambda}{2M}\right) - 2\pi. \end{aligned} \tag{3.26}$$

Substituting 3.14 into 3.26 we find,

$$\Delta\phi = \frac{6M}{l} + \frac{l^3\Lambda}{M}. \tag{3.27}$$

Our solution now takes the form

$$u = \frac{1}{l}[1 + \epsilon\cos(\omega\phi)], \tag{3.28}$$

where

$$\omega^2 = 1 - \frac{6M}{l} - \frac{l^3\Lambda}{M}. \tag{3.29}$$

Research suggests that Λ is a very small value around 2 x $10^{-35}s^{-2}$, therefore a plot of the orbits for the de Sitter - Schwarzschild solution look very similar to that of the Schwarzschild solution. Over a significant amount of time there would be a noticeable difference between them, however for a plot see figure 3.1.

3.3 The Post Newtonian Approximation

We will use [10] to find the approximate change in angle for our exact solution. We can use

$$\left(\frac{\mathrm{d}\chi}{\mathrm{d}\phi}\right)^2 = [(1 - 6\mu + 2\mu\epsilon) - 4\mu\epsilon\cos^2(\frac{1}{2}\chi)] \tag{3.30}$$

to find the first order correction to the orbits in Newtonian mechanics, known as Keplerian orbits. We note that $\mu = M/l$ is realistically an extrememly small number, taking a value around 2x10^{-6}. Therefore if we expand 3.30 we find

$$-\mathrm{d}\phi = \mathrm{d}\chi\,(1 + 3\mu + \mu\epsilon\cos\chi)\,, \tag{3.31}$$

which can be integrated to give

$$-\phi = (1 + 3\mu)\chi + \mu\epsilon\sin\chi + \text{constant}. \tag{3.32}$$

Therefore we see that the change in ϕ for one complete revolution, where χ changed by 2π, is $2\pi(1 + 3\mu)$. The advance in perihelion is therefore

$$\Delta\phi = 6\pi\frac{M}{l} = 6\pi\frac{M}{a(1-\epsilon^2)}, \tag{3.33}$$

where we have used 3.14 to remove the latus rectum. We note that 2.35 is exactly the same as 3.15.

Chapter 4

The Reissner-Nordström Solution

The Reissner-Nordström metric is a spherically symmetric solution for the coupled equations of Einstein and of Maxwell. This metric represents a black hole with the usual mass M, but includes a charge Q_*, as described in [11]. Since it is unlikely for a large body to possess a net charge, charged black holes are likely to be outside what is observationally possible. However the Reissner-Nordström solution is of interest due to the fact it has two event horizons, an external event horizon similar to a standard black hole, and an internal event horizon known as a Cauchy horizon. It is theorised that due to these two horizons, it is possible to pass into another universe through something known as a worm hole.

The Reissner-Nordström metric follows as,

$$ds^2 = \left(1 - \frac{2M}{r} + \frac{Q_*^2}{r^2}\right) dt^2 - \left(1 - \frac{2M}{r} + \frac{Q_*^2}{r^2}\right)^{-1} dr^2 - r^2 \left(d\theta^2 + \sin^2\theta d\phi^2\right). \quad (4.1)$$

This is similar to 2.3 only our $F(r)$ from 2.2 now becomes

$$F(r) = 1 - \frac{2M}{r} + \frac{Q_*^2}{r^2}. \quad (4.2)$$

Once again we set $\phi = \pi/2$ which gives us the same Lagrangian as 2.7. Working through similar to 2.7 to 2.15, with $L = -1/2$ for time-like particles, we obtain the geodesic equation

$$\left(\frac{\mathrm{d}u}{\mathrm{d}\phi}\right)^2 = -Q_*^2 u^4 + 2Mu^3 - u^2\left(1 + \frac{Q_*^2}{\ell^2}\right) + \frac{2M}{\ell^2}u - \frac{1 - E^2}{\ell^2} = f(u). \quad (4.3)$$

By setting $L = 0$ we find an equation for the null geodesics to be

$$\left(\frac{\mathrm{d}u}{\mathrm{d}\phi}\right)^2 = -Q_*^2 u^4 + 2Mu^3 - u^2 + \frac{1}{D^2} = f(u), \quad (4.4)$$

where $D = \ell/E$ is once again our impact parameter.

We now define Δ to be

$$\Delta = r^2 F(r) = r^2 - 2Mr + Q_*^2, \quad (4.5)$$

where the two roots of $\Delta = 0$ are,

$$r_+ = M + \sqrt{(M^2 - Q_*^2)} \quad \text{and} \quad r_- = M - \sqrt{(M^2 - Q_*^2)}. \tag{4.6}$$

These roots are real and distanct provided $M^2 > Q_*^2$. We can see that

$$\Delta > 0 \quad \text{for} \quad r > r_+ \quad \text{and} \quad 0 < r < r_-, \text{and} \quad \Delta < 0 \quad \text{for} \quad r_- < r < r_+. \tag{4.7}$$

The physical interpretation of these roots follows as; r_+ is an event horizon similar to that of the standard Schwarzschild radius $r = 2M$, and r_- is a horizon of a different type, known as the Cauchy horizon. For an observer who passed through the horizon of a charged black hole, at r_+, there are an infinite range of experiences and possibilities to be had, compared to an unfortunate observer who passed the corresponding event horizon for a black hole in Schwarzschild geometry, whose only option appears to be desolation at the singularity.

We must now distinguish three regions,

$$A: \quad 0 < r < r_-; \quad B: r_- < r < r_+ \quad \text{and} \quad C: r > r_+. \tag{4.8}$$

Region A is inside the Cauchy horizon, this is what we previously called a worm hole. Region B is in between the event horizon and the Cauchy horizon, this area is the same as for a Schwarzschild black hole. Region C is the area outside of the event horizon, more commonly known as the Universe. Each of the three regions has a parallel region, A', B' and C', which are obtained by applying a transformation which reverses the light-cone structure. A' represents a similar worm hole leading to B' in a similar way to A. B' represents a white hole which is the opposite of a black hole, nothing from the outside universe can pass its event horizon, although it behaves like any other mass in Schwarzschild geometery capable of having orbits. C' is a parallel universe, coexisting next to the universe C.

An observer who had already passed $r = r_+$ and followed a path across the surface $r = r_-$ would witness a flash containing a panorama of the entire history of the external universe. However, this flash would be extremely blue shifted as $\mathrm{d}t/\mathrm{d}\tau = -\infty$ for $r = r_-$. Once the observer passed back through the Cauchy horizon into B' they would witness a flash containing the entire future of their previous universe C_1. The observer is now in white hole, which fortunately allows them to escape at $r = r_+$. At this boundary the observer would once again witness a flash containing the entire history of their new universe C_2. In Figure 4.1 we give a pictoral indication of how this process would work.

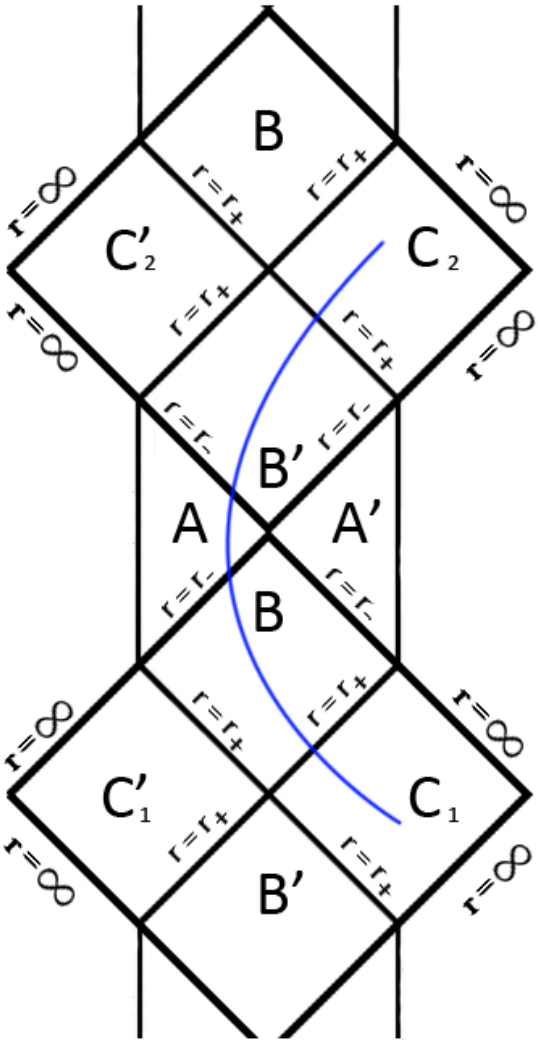

Figure 4.1: A Penrose diagram showing the maximum analytic extension of Reissner-Nordström space-time. The diagram can be extended to inifinity in either direction, with this just being a small section, to ensure that all geodesics can continue both in the past and future directions. I have labelled my universes C_1 and C_2 to highlight that they are different. This is because an observer which travels from C_1 to C_2, as the blue line indicates, can not enter their own universe once $r = r_+$ has been passed, without re-entering a different worm hole and hoping to end up back in C_1. This is not to be advised.

4.1 The Null Geodesics

We will now use [12] consider orbits for null particles, ie when $L = 0$. We can see that 4.4 always allows for two real roots when the quartic equation $f(u) = 0$. One root will be negative and has no physical significance, and one will be positive which occurs for $r < r_-$. We will only be interested in cases where the two remaining roots are real. We let the value of the impact parameter, D, which allows $f(u) = 0$ to have a double root to be known as D_c.

For all values of $D > D_c$ we have orbits of both first and second kind, similar to Schwarzschild space-time. Orbits of the first kind will be entirely outside of the event horizon, come from $+\infty$ and return to $+\infty$ after a perihelion passage. Orbits of the second kind have two turning points, one outside the event horizon ($r = r_+$) and one

inside the Cauchy horizon ($r < r_-$).

For values of $D < D_c$ we see that $f(u) = 0$ allowes only one real root, therefore orbits coming for $+\infty$ will cross both horizons and have a turning point for $r < r_-$ meaning that all thes orbits miss the singularity at $r = 0$. This turning point does not indicate that the orbit returns upon itself back into the area $r_- < r < r_+$, but instead travels through $A \to B' \to C_2$.

Using 4.4,

$$f(u) = -Q_*^2 u^4 + 2Mu^3 - u^2 + \frac{1}{D^2} = 0, \tag{4.9}$$

we differentiate to find

$$f'(u) = -2u\left(2Q_*^2 u^2 - 3Mu^3 + 1\right) = 0. \tag{4.10}$$

We see that $u = 0$ is a root, however we are more interested in the roots

$$u = \frac{3M}{4Q_*^2}\left[1 \pm \left(1 - \frac{8Q_*^2}{9M^2}\right)^{\frac{1}{2}}\right]. \tag{4.11}$$

The larger of these roots maximises $f(u)$ and we know the double root we search for must occur at a minimum. This gives us a critical value of u,

$$u = u_c = \frac{3M}{4Q_*^2}\left[1 - \left(1 - \frac{8Q_*^2}{9M^2}\right)^{\frac{1}{2}}\right], \tag{4.12}$$

and the corresponding value of r is

$$r_c = \frac{3}{2}\left[1 + \left(1 - \frac{8Q_*^2}{9M^2}\right)^{\frac{1}{2}}\right]. \tag{4.13}$$

At this radius, r_c, the geodesics allow unstable circular orbits.

Substituting 4.13 into 4.4 results in a critical impact parameter, D_c, which follows as

$$D_c = \frac{r_c^2}{\sqrt{\Delta_c}} \quad \text{where} \quad \Delta_c = r_c^2 - 2Mr_c + Q_*^2 = Mr_c - Q_*^2. \tag{4.14}$$

If we now set $D = D_c$ in 4.4 we find

$$f(u) = (u - u_c)^2\left[-Q_*^2 u^2 + 2u(M - Q*^2 u_c) + u_c(M - Q_*^2 u_c)\right], \tag{4.15}$$

and therefore our solution for ϕ is given as

$$\phi = \pm \int \left[-Q_*^2 u^2 + 2u(M - Q*^2 u_c) + u_c(M - Q_*^2 u_c)\right]^{-\frac{1}{2}} \frac{\mathrm{d}u}{u - u_c}. \tag{4.16}$$

Using a substitution, given in [12],

$$\xi = (u - u_c)^{-1}, \tag{4.17}$$

reduces 4.16 to

$$\phi = \mp \int \frac{\mathrm{d}\xi}{(-Q_*^2 + b\xi + c\xi^2)}, \tag{4.18}$$

where

$$b = 2\left(M - 2Q_*^2 u_c\right) \quad \text{and} \quad c = u_c\left(3M - 4Q_*^2 u_c\right). \tag{4.19}$$

We therefore integrate 4.18 to obtain our solution

$$\mp\phi = \begin{cases} \frac{1}{\sqrt{c}} \ln\left[2\left(c\left(-Q_*^2 + b\xi + c\xi^2\right)\right)^{\frac{1}{2}} + 2c\xi + b\right] \text{for } \ c > 0, \\ \\ -\frac{1}{\sqrt{-c}} \sin^{-1}\left[\frac{2c\xi + b}{(4Q_*^2 c + b^2)^{\frac{1}{2}}}\right] \text{for } \ c < 0. \end{cases} \tag{4.20}$$

This solution describes both orbits of the first and second kind, however they only exist in the ranges:

$$\infty > r > r_c, \quad 0 \leq u \leq u_c \quad \text{and} \quad -u_c^{-1} > \xi > -\infty, \tag{4.21}$$

for orbits of the first kind, and

$$r_c > r > r_{\min}, \quad u_c < u \leq u_{\max} \quad \text{and} \quad \infty > \xi > \xi_{\min}, \tag{4.22}$$

for orbits of the second kind. Where $\xi_{\min} = (u_{\min} - u_c)^{-1}$ and $u_{\max} = 1/r_{\min}$, and $r_{\min}$ is the positive root of the equation

$$u_c\left(M - Q_*^2 u_c\right) r^2 + 2\left(M - Q_*^2 u_c\right) r - Q_*^2 = 0. \tag{4.23}$$

Therefore

$$r_{\min} = -r_c + \sqrt{\frac{M r_c^2}{M - Q_*^2 u_c}}. \tag{4.24}$$

We can see an example of this orbit in Figure 4.2.

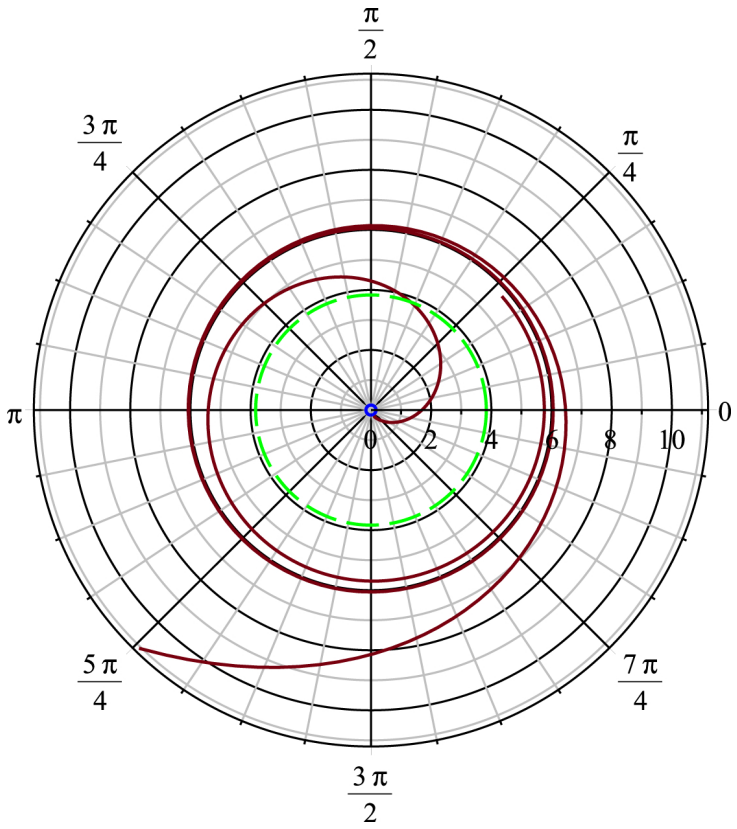

Figure 4.2: Orbits of the first and second kind for a null test particle in Reissner-Nordström space time. We have set $M = 2$ and $Q_* = 0.8$, giving us a positive value for c and our impact parameter $D_c \approx 10.1$. We therefore use the logarithmic equation for ϕ. We can see that the particle originally comes in from infinity, and orbits the black hole an infinite number of times at the critical distance $r_c \approx 5.8$. It then changes direction and orbits towards the singularity passing through the event horizon at $r = 3.83$ and eventually terminates just as it hits the cauchy horizon at $r = 0.16$. It does not go to the singularity at $r = 0$. Distances have been scaled in terms of the Schwarzschild radius.

4.2 The Time-Like Geodesics

We will now consider the time-like geodesics for the Reissner-Nordström solution, using [13]. We can see that Δ in 4.5 is greater than zero in the interval $0 \leq r < r_-$, therefore $E^2r^2 - \Delta$ will disappear for some value in $0 \leq r < r_-$. This leads us to the conclusion that there is a turning point somewhere within the Cauchy horizon, meaning that the time-like geodesics do not reach the singularity, similar to the null geodesics. They will avoid the singularity and end up in other domains, through the same process as seen for null particles.

Restating 4.3,

$$\left(\frac{\mathrm{d}u}{\mathrm{d}\phi}\right)^2 = -Q_*^2u^4 + 2Mu^3 - u^2\left(1 + \frac{Q_*^2}{\ell^2}\right) + \frac{2M}{\ell^2}u - \frac{1-E^2}{\ell^2} = f(u), \tag{4.25}$$

we see that the condition for circular orbits are

$$f(u) = -Q_*^2u^4 + 2Mu^3 - u^2\left(1 + \frac{Q_*^2}{\ell^2}\right) + \frac{2M}{\ell^2}u - \frac{1-E^2}{\ell^2} = 0, \tag{4.26}$$

and

$$f'(u) = -4Q_*^2u^3 + 6Mu^2 - 2u\left(1 + \frac{Q_*^2}{\ell^2}\right) + \frac{2M}{\ell^2} = 0. \tag{4.27}$$

Using these equations, we can show that the angular momentum ℓ and energy E of a circular orbit at radius r_c are

$$\ell^2 = \frac{M - Q_*^2u_c}{u_c\left(1 - 3Mu_c + 2Q_*^2u_c^2\right)} \tag{4.28}$$

and

$$E^2 = \frac{\left(1 - 2Mu_c + Q_*^2u_c^2\right)^2}{1 - 3Mu_c + 2Q_*^2u_c^2}. \tag{4.29}$$

It is obvious from these equations that we need $1-3Mu_c+2Q_*^2u_c^2 > 0$. If we compare this inequality to 4.10 we can that the radius for an unstable circular orbit of a null geodesic is the same as the minimum radius for a time-like circular orbit. When E and ℓ have the values from 4.28 and 4.29, which are appropriate for a circular orbit of radius $r_c = 1/u_c$, the equation 4.3 becomes

$$f(u) = (u - u_c)^2\left[-Q_*^2u^2 + 2u(M - Q*^2u_c) + u_c\left(M - Q_*^2u_c - \frac{M}{\ell^2u_c^2}\right)\right]. \tag{4.30}$$

We see that, besides the obvious circular orbits at $r_c = 1/u_c$, we get orbits of the second kind determined by

$$\phi = \pm\int\left[-Q_*^2u^2 + 2u(M - Q*^2u_c) + u_c\left(M - Q_*^2u_c - \frac{M}{\ell^2u_c^2}\right)\right]^{-\frac{1}{2}}\frac{\mathrm{d}u}{u - u_c}. \tag{4.31}$$

This is very similar to equation 4.16 so once again we use the substitution

$$\xi = (u - u_c)^{-1}, \tag{4.32}$$

we arrive at the same solution,

$$\mp\phi = \begin{cases} \frac{1}{\sqrt{c}}\ln\left[2\left(c\left(-Q_*^2 + b\xi + c\xi^2\right)\right)^{\frac{1}{2}} + 2c\xi + b\right] \text{ for } \ c > 0, \\ \\ -\frac{1}{\sqrt{-c}}\sin^{-1}\left[\frac{2c\xi+b}{(4Q_*^2c+b^2)^{\frac{1}{2}}}\right] \text{ for } \ c < 0. \end{cases} \tag{4.33}$$

with the slight differences in that,

$$b = 2\left(M - 2Q_*^2u_c\right) \quad \text{and} \quad c = u_c\left(3M - 4Q_*^2u_c - \frac{M}{\ell^2u_c^2}\right). \tag{4.34}$$

We can see an example of this orbit in Figure 4.3.

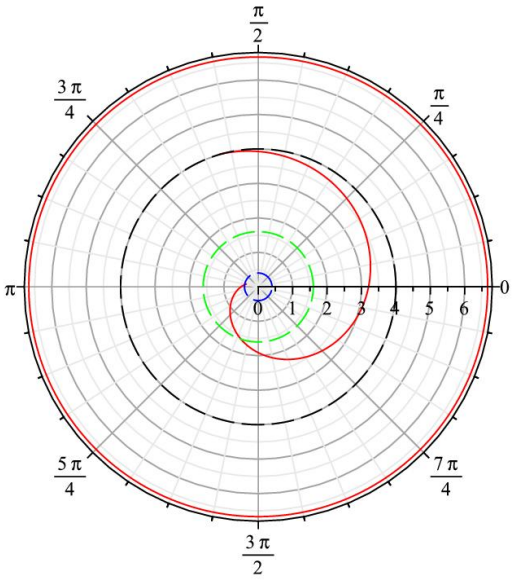

Figure 4.3: The stable orbit for time-like particles with $M = 1$ and $Q_* = 0.8$. The circular red line at $r_c = 6.67$ indicates the stable orbit of the first kind. The spiralling red line indicates the orbit of the second kind, which starts at $r = 4$, passes through the event horizon at $r = 1.6$ and terminates just after passing the Cauchy horizon at $r = 0.4$, indicated repectively by the dashed black, green and blue lines. Distances have been scaled in terms of the Schwarzschild radius.

We can now search for the minimum radius for a stable orbit. We know that this occurs at a point of inflection of $f(u)$, therefore we differentiate 4.26 twice, giving us

$$f''(u) = -12Q_*^2u^2 + 12Mu - 2\left(1 + \frac{Q_*^2}{\ell^2}\right) = 0. \tag{4.35}$$

Substituting 4.28 into this equation to eliminate ℓ^2 and rearranging, gives

$$4Q_*^4u_c^3 - 9MQ_*^2u_c^2 + 6M^2u_c - M = 0, \tag{4.36}$$

which can be rewritten as,

$$r_c^3 - 6Mr_c^2 + 9Q_*^2r_c - 4\frac{Q_*^4}{M} = 0. \tag{4.37}$$

We can see that if we choose $Q_* = 0$ in 4.37, we get that $r_c = 6M$ which agrees with Schwarzchild geometry.
When all three of 4.26, 4.27 and 4.37 are satisfied we find that 4.3 takes the form

$$\left(\frac{\mathrm{d}u}{\mathrm{d}\phi}\right)^2 = (u - u_c)^3\left(2M - 3Q_*^2u_c - Q_*^2u\right), \tag{4.38}$$

and our solution takes the form

$$u = u_c + \frac{2\left(M - 2Q_*^2u_c\right)}{\left(M - 2Q_*^2u_c\right)^2(\phi - \phi_0)^2 + Q_*^2}. \tag{4.39}$$

We can see an example of this orbit in Figure 4.4.

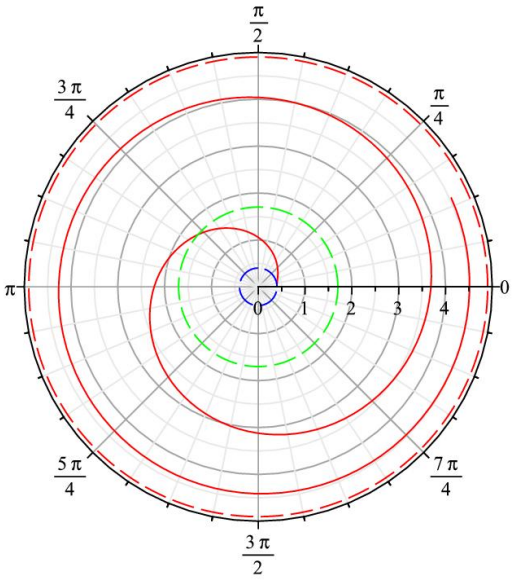

Figure 4.4: The last time-like unstable orbit with $M = 1$ and $Q_* = 0.8$. The solid red line indicates our orbit which approaches from our dashed red line at $r_c = 4.89$, which indicates the last stable orbit. It passes through the event horizon at $r = 1.6$ and eventually terminates just inside the Cauchy horizon at $r = 0.4$, indicated repectively by the dashed green and blue lines. Distances have been scaled in terms of the Schwarzschild radius.

Chapter 5

Conclusion

In this report we used Einstein's general theory of relativity to describe the behaviour of a particle outside a black hole. We found the exact solutions for orbits of the first and second kind, for the bound and unbound orbits, of time-like and null particles using the Schwarzschild metric. We then considered the approximate solutions to the Schwarzschild and the de Sitter-Schwarzschild metrics, and used the post Newtonian approximation to compare these to our exact solution. Finally we discussed the Reissner-Nordström metric and its properties that allow two event horizons and travelling between universes through worm holes.

If we were to have more time available to continue this report an area of interest would have been to include a solution to the Kerr and Kerr-Newman metrics. The Kerr solution allows for a rotating black hole, and the Kerr-Newman solution allows for a rotating, charged black hole. These orbits are of interest as they exhibit an effect known as frame-dragging, which states that the gravitational field of the body is not only dependent on its mass, but also on its rotation. These effects were one of the the main focus points for the gravity probe B experiment, which was also a a fantastic test of general relativity.

Another direction we could take if more time were available would be to look into orbiting bodies made of multiple particles, instead of the single point particles which have been considered in this report. For this we would be required to created a computer simulation in a program like Fortran. With this we could simulate bodies ranging from organic life all the way up to galaxies. It would be interesting to see how bodies such as stars are pulled apart by black holes, and make comparisons between the simulation and observational evidence. An example of this observational evidence happened in 2011 when Sagittarius A*, a super massive black hole believed to be at the centre of the Milky Way (as seen in [14]), stretching out a gas cloud known as G2.

Bibliography

[1] D.J. Toms (2004-2006), *Relativity*, Newcastle University, pp. 71-75.

[2] R.M. Wald (1997), *Gravitational Collapse and Cosmic Censorship.*

[3] D. Finkelstein (1958), *Past-Future Asymmetry of the Gravitational Field of a Point Particle*, Physical Review 110 (4): 965-967.

[4] S. Chandrasekhar (1983), *The Mathematical Theory of Black Holes*, Oxford University press, pp. 96 - 108.

[5] S. Chandrasekhar (1983), *The Mathematical Theory of Black Holes*, Oxford University press, pp. 106 -107 and pp.109-110.

[6] S. Chandrasekhar (1983), *The Mathematical Theory of Black Holes*, Oxford University press, pp. 113 - 115.

[7] S. Chandrasekhar (1983), *The Mathematical Theory of Black Holes*, Oxford University press, pp. 123 - 127.

[8] S. Chandrasekhar (1983), *The Mathematical Theory of Black Holes*, Oxford University press, pp. 130-133.

[9] D.J. Toms (2004-2006), *Relativity*, Newcastle University, pp. 76-78.

[10] S. Chandrasekhar (1983), *The Mathematical Theory of Black Holes*, Oxford University press, pp. 107 -108.

[11] S. Chandrasekhar (1983), *The Mathematical Theory of Black Holes*, Oxford University press, pp. 209-216.

[12] S. Chandrasekhar (1983), *The Mathematical Theory of Black Holes*, Oxford University press, pp. 216 -219

[13] S. Chandrasekhar (1983), *The Mathematical Theory of Black Holes*, Oxford University press, pp. 219 -223.

[14] M. Henderson (2008), *Astronomers confirm black hole at the heart of the Milky Way*, Times Online.